RAA 2020 Vol. **20** No. **4**, 50(8pp) doi: 10.1088/1674–4527/20/4/50
© 2020 National Astronomical Observatories, CAS and IOP Publishing Ltd.
http://www.raa-journal.org *http://iopscience.iop.org/raa*

***R**esearch in*
***A**stronomy and*
***A**strophysics*

New multi-color photometric investigations of solar-like contact binary V680 Per

Jing-Jing Wang[1,3], Jia-Jia He[2,3] and Song-Qing Zhao[1]

[1] China University of Petroleum–Beijing at Karamay, Karamay 834000, China; *wangjingjing@cupk.edu.cn*
[2] Yunnan Observatories, Chinese Academy of Sciences, Kunming 650216, China
[3] Key Laboratory of the Structure and Evolution of Celestial Objects, Chinese Academy of Sciences, Kunming 650216, China

Received 2019 November 15; accepted 2020 December 18

Abstract High-precision CCD photometric observations of the contact binary V680 Per were obtained in 2016. Its symmetric multi-color light curves were analyzed by using the Wilson–Devinney (2013) program. These photometric solutions suggest that V680 Per is an A-type W UMa contact binary with the mass ratio of q=0.693 and a fill-out factor of $f = 18.84\%$ with a small temperature difference of 101 K. Based on all minimum times, the $O - C$ curve was analyzed for the first time in this study. A cyclic oscillation ($A_3 = 0.00093\,$d, $T_3 = 4.92\,$yr) superimposed on a secular decrease ($dP/dt = -8.16 \times 10^{-8}\,$d yr^{-1}) was identified. The continuous decrease in period is possibly a result of mass transfer from the more massive component to the less massive one, or angular momentum loss due to a magnetic stellar wind. Because of this secular decrease, it is predicted that the degree of contact will become higher, and V680 Per will evolve into a deeper overcontact binary.

Key words: binaries : eclipsing — stars: solar-type stars: individual (V680 Per)

1 INTRODUCTION

W UMa-type eclipsing binaries usually consist of two ellipsoidal FGK dwarfs, the components of which fill their critical Roche lobes, and sharing a common convective envelope (CCE). Thanks to plentiful photometric and spectroscopic data, a large number of these systems were discovered from survey projects, such as: LAMOST (Qian et al. 2017), OGLE (Rucinski 1997), Catalina Sky Survey (Drake et al. 2009 and ASAS (Gettel et al. 2006). Statistical studies show that most W UMa-type binaries are solar-type main-sequence stars that undergo the proton-proton (p-p) chain nuclear reaction in their stellar cores. However, the formation and evolution of W UMa contact binaries are still unclear. Some investigators assumed these binaries form from short-period detached binaries through angular momentum loss (Guinan & Bradstreet 1988; Bradstreet & Guinan 1994; Zhu et al. 2004; Zhu & Qian 2006). Also, the third bodies may play a significant role in the origin of contact binaries by removing angular momentum from the central binary through early dynamical interaction and/or later evolution (Qian et al. 2014b; Zhu et al. 2013b). To understand these, it is necessary to study low mass solar-type binaries and their additional companions.

V680 Per (= GSC 2336 0281) is a W UMa contact binary discovered by Zejda (2002), the orbital period of which was found to be 0.3739783 d. Samec et al. (2005) analyzed $UBVR_cI_c$-band light curves, and concluded that V680 Per is a W-type W UMa binary with a temperature difference of about 100 K and a cool spot on the more massive, cooler component. Up to now, the orbital period investigation of this system was ignored. There are some CCD minimum times from literatures that were recorded during the last 17 yr, and we obtained new higher precision light curves. In this paper, orbital period variations of V680 Per are analyzed and the corresponding photometric solution is re-obtained. Based on the properties of period change and derived parameters, the ternary nature, evolution and configuration are discussed.

2 OBSERVATIONS

The four-color photometric observations of V680 Per were carried out in two nights on January 11 and 13 in 2016, with the 1024×1024 PI1024 BFT CCD

Table 1 Coordinates of the Contact Binary V680 Per (V), and the Comparison (C) and Check Stars (Ch).

Stars	α_{2000}	δ_{2000}	$V_{\rm mag}$
V680 Per (V)	$02^{\rm h}41^{\rm m}41^{\rm s}$	$+35^\circ42'54''.9$	13.49
TYC 2336–5891 (C)	$02^{\rm h}41^{\rm m}57^{\rm s}$	$+35^\circ45'59''.5$	10.06
TYC 2336–2411 (Ch)	$02^{\rm h}41^{\rm m}31^{\rm s}$	$+35^\circ49'06''.8$	10.77

camera attached to the 85-cm telescope at Xinglong Station of National Astronomical Observatories, Chinese Academy of Sciences. The effective field of view was 16.5 arcmin×16.5 arcmin, and the filter system was a standard Johnson-Cousins-Bessel multi-color CCD photometric system mounted at the primary focus (Zhou et al. 2009). The integration times were 20 s for B band, 15 s for V band, 10 s for R_c band and 8 s for I_c band. The variable (V), comparison star (C) and check star (Ch) are shown in Figure 1, and their coordinates and magnitudes are listed in Table 1. In observations, we used differential photometry to obtain light curves of V680 Per which are displayed in the upper panel of Figure 2. The PHOT task in the IRAF aperture photometry package was applied to reduce the observed images, including a flat field correction process (Kallrath & Milone 1999). The mean photometric errors for individual observations are 0.0020 mag in the BI_c band and 0.0015 mag in VR_c band.

With the linear ephemeris equation,

$$\text{Min.I (HJD)} = 2457401.0543 + 0^{\rm d}.37422033 \times E, \quad (1)$$

the BVR_cI_c light curves along with their magnitudes and phases are displayed in Figure 2. In the lower panel of Figure 2, the differential magnitudes between the comparison star (C) and check star (Ch) are almost stable, which hints that the observational conditions are good. From our new observations, we can see that the light curves of V680 Per are nearly symmetric, and belong to the EW-type. These curves allow us to obtain more reliable photometric solutions.

To get more times of light minimum, we also monitored it with the 60-cm and 1.0-m telescopes managed by Yunnan Observatories (YNO). These two telescopes were equipped with the same Cassegrain-focus multicolor CCD photometer, where an Andor DW436 2K CCD camera was employed. These CCD times of minimum light were determined and are listed in Table 2.

3 VARIATIONS OF THE $O-C$ DIAGRAM

The orbital period changes are one important tool to understand the evolution of contact binary stars, for example, AL Cas (Qian et al. 2014a), LU Lac (Liao et al. 2014) and RV Psc (He & Qian 2009). Since V680 Per was discovered in 2002 (Zejda 2002), there are some CCD times of minimum light, without visual or photographic ones. Considering the technology implemented in a CCD and some times of minimum without errors, we assigned the same weight to these times to describe the trend of the $O-C$ (Sterken 2005). In our present work, all available times of minimum light are collected. Minimum times with the same epoch have been averaged, and only the mean values are listed in Table 2.

By using the ephemeris expressed in Equation (1), we calculated the $(O-C)_1$ values, which are plotted in the upper panel of Figure 3. To explore the variations in $(O-C)_1$, we performed some tests such as linear ephemeris term, parabolic term, cyclic term and parabolic plus cyclic term to fit all of these data. The residuals of the different fittings are listed in Table 3, suggesting the cyclic plus parabolic ephemeris to be reliable.

Based on the least-squares method, a cyclic plus parabolic term yields the following equation (Sterken 2005; Irwin 1952),

$$T = T_0 + P_0E + \frac{1}{2}\frac{dP}{dt}PE^2 + A_3\sin(\omega E + \phi), \quad (2)$$

where A_3 is the amplitude of the sinusoidal variation, T_3 the period of the cycle, $\omega(=\frac{360^\circ}{T_3}P)$ the angle per unit epoch and ϕ the phase. We obtained the new ephemeris

$$\begin{aligned}\text{Min.I (HJD)} = {} & 2457401.0534(\pm0.0002)\\ & + 0.^{\rm d}37421962(\pm0.00000007) \times E\\ & - 4.18(\pm0.49) \times 10^{-11} \times E^2\\ & + 0.00093(\pm0.00019)\sin[0^\circ.075022 \times E\\ & + 77^\circ.74(\pm14^\circ.30)].\end{aligned} \quad (3)$$

As displayed in the upper panel of Figure 3, the general trend of the $(O-C)_1$ curve manifests a downward parabolic change, indicating that the period is continuously decreasing. After the long-term decrease was removed from the $(O-C)_1$ curve, we found there is a periodic variation displayed in the middle of Figure 3.

The parabolic term in this ephemeris indicates a long-term period decrease at a rate of $dP/dt = -8.16 \times 10^{-8}\,\mathrm{d\,yr^{-1}}$. In the middle panel, the red solid line represents the oscillation with an amplitude of 0.00093 d and a period of 4.92 yr. The corresponding residuals from the whole fitting are displayed in the lower panel of Figure 3.

4 PHOTOMETRIC SOLUTIONS WITH THE WILSON-DEVINNEY PROGRAM

By modeling with Binary Maker 2.0, the preliminary solutions from Samec et al. (2005) revealed that the system was a W-type, W UMa binary with $q = M_2/M_1 = 0.418$, and a temperature difference of $\Delta T = T_1 - T_2 =$

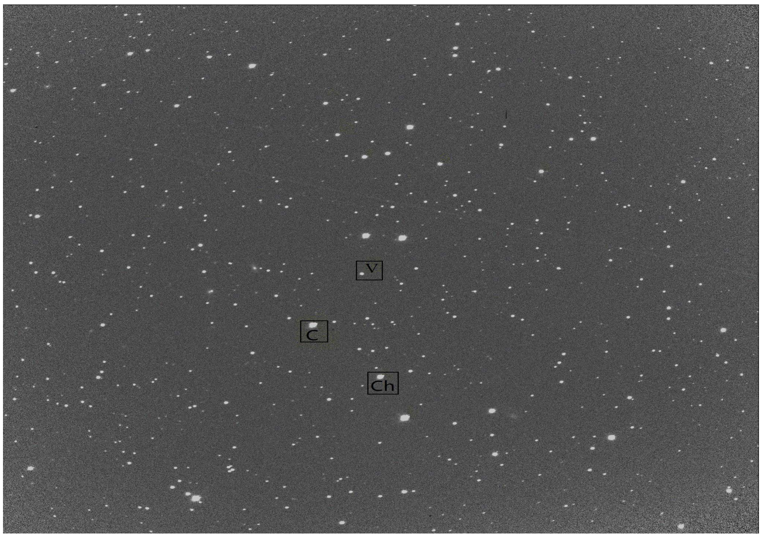

Fig. 1 Observed CCD images of V680 Per (V), and the comparison (C) and check stars (Ch).

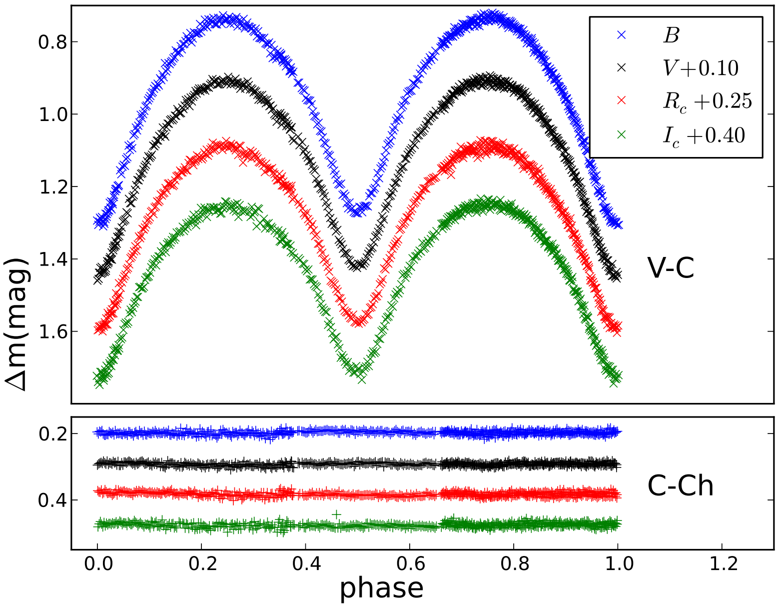

Fig. 2 *Upper*: BVR_cI_c-band observations of V680 Per in 2016, with 85-cm telescope at Xinglong Station. For each subgraph: *blue* refers to the B-band magnitudes of the variable star minus the comparison star (V-C), *black* to the V-band, *red* to the R_c-band and *green* to the I_c-band. Lower: BVR_cI_c-band magnitudes of the comparison star minus the check star (C-Ch).

$5500\,\mathrm{K} - 5608\,\mathrm{K} = -108\,\mathrm{K}$. To account for intercomponent mass flow or streaming in the “neck” of the Roche Lobe, we also added a cool spot on the more massive, cooler component. Our higher precision observations shown in Figure 2 are typical for EW-type variations as these light curves are from Samec et al. (2005). The depths between the primary and secondary minima are nearly the same. Besides, because the heights between two maxima are equal, there is no obvious O’Connell effect. In order to investigate the magnetic activities and understand their evolution, we intend to analyze the present multi-color light curves that were acquired in 2016. The photometric solutions are derived with the Wilson-Devinney program (W-D), version 2013 (Wilson & Devinney 1971; Wilson 1979; Wilson 1990; Van Hamme & Wilson 2007; Wilson 2008).

According to the LAMOST spectral type of F5V, the temperature was fixed to be $T = 6140\,\mathrm{K}$ in 2012 and $T = 6067\,\mathrm{K}$ in 2016 (Qian et al. 2017), so we took the

Table 2 $O-C$ Values of Light Minimum Times for V680 Per

HJD	Epoch	$(O-C)_1$	$(O-C)_2$	Residuals	Errors	Ref.
2451550.3066	–15634.5	0.000049	–0.000704	–0.001089	0.0031	Zejda (2002)
2451576.3166	–15565.0	0.001736	0.000962	0.000454	0.0045	Zejda (2002)
2451771.4714	–15043.5	0.000634	–0.000287	0.000002	0.0055	Zejda (2002)
2451841.4510	–14856.5	0.001033	0.000062	0.000636	0.0019	Zejda (2002)
2451841.6388	–14856.0	0.001722	0.000752	0.001326	0.0014	Zejda (2002)
2451876.4423	–14763.0	0.002732	0.001737	0.002281	0.0016	Zejda (2002)
2452995.7337	–11772.0	0.001125	–0.000438	–0.000944	0.0003	Faulkner et al. (2004)
2452996.6688	–11769.5	0.000674	–0.000889	–0.001399	0.0006	Faulkner et al. (2004)
2451924.3389	–14635.0	–0.000870	–0.001898	–0.00157	0.0020	Zejda (2004)
2452133.5310	–14076.0	0.002065	0.000904	0.000432	0.0018	Zejda (2004)
2452138.5820	–14062.5	0.001091	–0.000074	–0.000522	0.0024	Zejda (2004)
2452147.5654	–14038.5	0.003203	0.002033	0.001631	0.0033	Zejda (2004)
2452198.4573	–13902.5	0.001138	–0.000062	–0.000115	0.0033	Zejda (2004)
2452198.6443	–13902.0	0.001028	–0.000172	–0.000224	0.0036	Zejda (2004)
2452213.4252	–13862.5	0.000225	–0.000984	–0.000922	0.0049	Zejda (2004)
2452213.6141	–13862.0	0.002014	0.000806	0.000869	0.0030	Zejda (2004)
2452521.5980	–13039.0	0.002583	0.001211	0.000708	0.0020	Zejda (2004)
2452524.5904	–13031.0	0.001220	–0.000153	–0.000667	0.0035	Zejda (2004)
2452229.3309	–13820.0	0.001561	0.000343	0.000524	0.0042	Zejda (2004)
2452229.5196	–13819.5	0.003150	0.001933	0.002115	0.0040	Zejda (2004)
2452234.5703	–13806.0	0.001876	0.000655	0.000874	0.0032	Zejda (2004)
2452900.4943	–12026.5	0.000799	–0.000731	–0.000617	0.0038	Zejda (2004)
2452999.8481	–11761.0	–0.000899	–0.002463	–0.002984	0.0004	Samec et al. (2005)
2452999.6624	–11761.5	0.000511	–0.001052	–0.001573	0.0008	Samec et al. (2005)
2453290.6198	–10984.0	0.001605	–0.000040	0.000518	0.0003	Zejda et al. (2006)
2453713.3030	–9854.5	0.002942	0.001229	0.001761	0.0004	Zejda et al. (2006)
2455543.6134	–4963.5	0.001708	0.000363	0.000553	0.0003	Diethelm (2011)
2453262.9265	–11058.0	0.000609	–0.001029	–0.000453	0.0002	Krajci (2006)
2454793.8643	–6967.0	0.003039	0.001413	0.001525	0.0002	Nelson (2009)
2454838.0219	–6849.0	0.002640	0.001025	0.000805	None	$O-C$ Gateway
2454843.0732	–6835.5	0.001966	0.000352	0.000096	None	$O-C$ Gateway
2455114.9429	–6109.0	0.000596	–0.000932	–0.000470	0.0006	Diethelm (2010)
2455119.8090	–6096.0	0.001832	0.000305	0.000789	0.0020	Diethelm (2010)
2455119.9950	–6095.5	0.000722	–0.000805	–0.000320	0.0002	Diethelm (2010)
2455121.8660	–6090.5	0.000620	–0.000906	–0.000413	0.0003	Diethelm (2010)
2455171.8248	–5957.0	0.001006	–0.000501	0.000074	0.0003	Nelson (2010)
2455847.8558	–4150.5	0.002980	0.001801	0.001256	0.0010	Diethelm (2012)
2455859.2671	–4120.0	0.000560	–0.000612	–0.001180	0.0015	Hubscher & Lehmann (2012)
2455859.4552	–4119.5	0.001549	0.000378	–0.000191	0.0010	Hubscher & Lehmann (2012)
2455894.2583	–4026.5	0.002159	0.001008	0.000452	0.0007	Hubscher & Lehmann (2012)
2455894.4451	–4026.0	0.001849	0.000698	0.000142	0.0012	Hubscher & Lehmann (2012)
2456214.9626	–3169.5	–0.000364	–0.001302	–0.001199	0.0003	Diethelm (2013)
2457301.1389	–267.0	0.001428	0.001456	0.000880	None	$O-C$ Gateway
2457301.3243	–266.5	–0.000282	–0.000254	–0.000829	None	$O-C$ Gateway
2457302.2624	–264.0	0.002267	0.002296	0.001722	None	$O-C$ Gateway
2457732.9881	887.0	0.000367	0.000885	0.000364	None	$O-C$ Gateway
2458037.2260	1700.0	–0.002861	–0.001962	–0.001441	None	$O-C$ Gateway
2455914.0914	–3973.5	0.001581	0.000443	–0.000054	0.0002	Present paper
2457021.0347	–1015.5	0.001145	0.000887	0.001402	0.0002	Present paper
2457398.9959	–5.5	–0.000188	–0.000055	–0.000152	0.0001	Present paper
2457399.1831	–5.0	–0.000098	0.000036	–0.000060	0.0002	Present paper
2457401.0543	0.0	0.000000	0.000136	0.000054	0.0001	Present paper
2458385.2497	2630.0	–0.004068	–0.002696	–0.002493	0.0002	Present paper
2458425.1047	2736.5	–0.003533	–0.000395	0.000511	0.0003	Present paper
2458455.0408	2816.5	–0.005059	–0.001846	–0.000966	0.0004	Present paper
2458457.1004	2822.0	–0.003671	-0.000452	0.000425	0.0009	Present paper
2458458.0332	2824.5	–0.006422	–0.003201	–0.002324	0.0003	Present paper

Table 3 Fitting Residuals of Different Ephemeris Terms for $(O-C)_1$

Linear	Parabolic	Cyclic	Parabolic+Cyclic
1.6803×10^{-6}	1.2497×10^{-6}	1.7261×10^{-6}	1.0484×10^{-6}

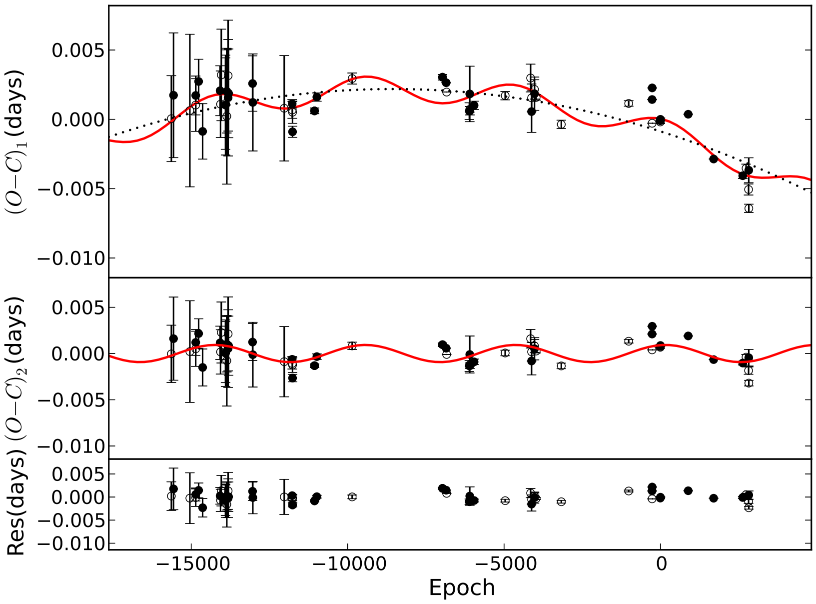

Fig. 3 The $O-C$ diagram for V680 Per. *Top panel*: the *dotted line* represents the quadratic trend and the *solid line* signifies the cyclic trend. *Middle panel*: the *solid line* corresponds to the cyclic change. *Bottom panel*: the residuals with respect to Equation (3).

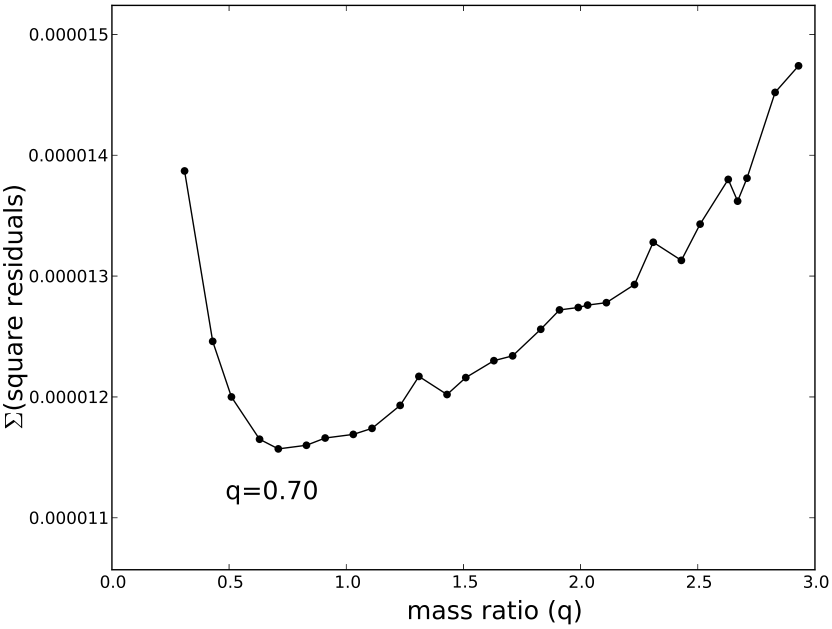

Fig. 4 Relation between Σ and q. The minimum residual is achieved at $q = 0.70$.

Table 4 Photometric Solutions of V680 Per

Parameters	Photometric elements	Errors	Parameters	Photometric elements	Errors
$g_1 = g_2$	0.32	Assumed	$L_1/(L_1 + L_2)\,(B)$	0.6051	±0.0005
$A_1 = A_2$	0.5	Assumed	$L_1/(L_1 + L_2)\,(V)$	0.5991	±0.0005
LD	–3	Assumed	$L_1/(L_1 + L_2)\,(R_c)$	0.5963	±0.0005
$x_{1\mathrm{bol}}$,$y_{1\mathrm{bol}}$	0.541,0.172	Assumed	$L_1/(L_1 + L_2)\,(I_c)$	0.5940	±0.0006
$x_{2\mathrm{bol}}$,$y_{2\mathrm{bol}}$	0.638,0.163	Assumed	r_1(pole)	0.3980	±0.0017
T_1	6104K	Assumed	r_1(side)	0.4225	±0.0022
T_2	6003K	$\pm5K$	r_1(back)	0.4573	±0.0033
q (M_2/M_1)	0.693	±0.006	r_2(pole)	0.3372	±0.0020
Ω_{in}	3.2007		r_2(side)	0.3547	±0.0025
Ω_{out}	2.8111		r_2(back)	0.3937	±0.0042
$\Omega_1 = \Omega_2$	3.1570	±0.0095	f	18.84%	$\pm2.38\%$
i	72.970	±0.049	$\Sigma\omega(O - C)^2$	0.0000124	

average temperature $T_1 = 6104\,\mathrm{K}$ for the primary star (star eclipsed at primary light minimum). Considering the convective atmospheres of the components, the same values of gravity-darkening coefficients and bolometric albedo, i.e., $g_1 = g_2 = 0.32$ (Lucy 1967) and $A_1 = A_2 = 0.5$ (Ruciński 1969), were considered in the model.

The complete BVR_cI_c-band light curves are applied to look for a suitable mass ratio $q = M_2/M_1$ (the secondary divided by the primary). The relation between the sum of squared residuals $\sum(\omega_i(O - C)_i)^2$ and q is displayed in Figure 4. The minimum in residuals is located at $q = 0.70$ with a Differential Correction (DC) code. When we applied mass ratio as an adjustable parameter to perform the differential corrections, the suitable mass ratio q converged at $q = 0.693$. The derived parameters listed in Table 4 indicate that V680 Per is an A-type shallow-contact binary without a spot. The theoretical light curves are displayed in Figure 5, and the configurations at phases 0.0, 0.25, 0.50 are 0.75 were modeled with the Light Curve (LC) code and displayed in Figure 6.

5 DISCUSSION AND CONCLUSIONS

The BVR_cI_c-band light curve recorded in 2016 was analyzed by employing the 2013 version of W-D program. These solutions suggest that V680 Per is a typical A-type contact binary with a degree of contact of $f = 18.84\%$, $q = M_2/M_1 = 0.693$ and temperature difference of $\Delta T = T_1 - T_2$ =6104 K–6003 K=101 K, where both components share a CCE without spot activities. Based on the spectral type, the more massive component is F5V (Qian et al. 2017), and its corresponding mass is estimat-

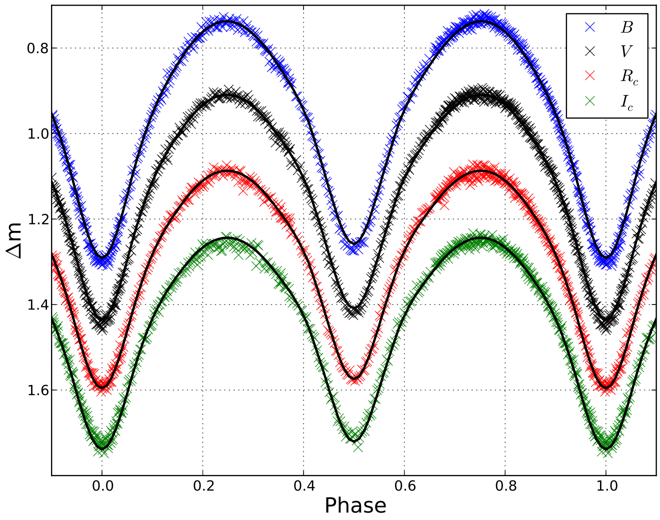

Fig. 5 Observed (×) and theoretical (*line*) light curves calculated with the W-D (2013) program.

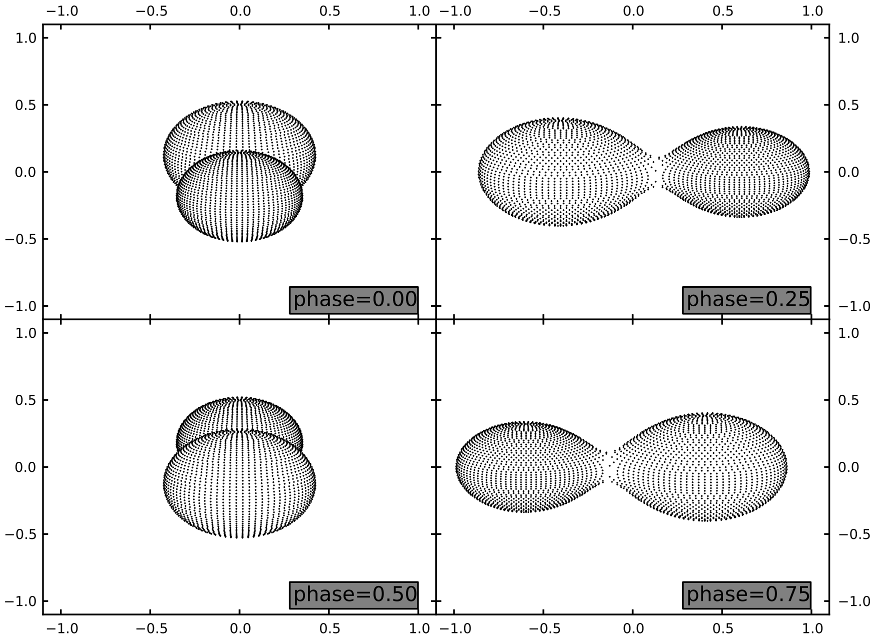

Fig. 6 Geometric configurations of V680 Per at phases 0.00, 0.25, 0.50 and 0.75.

ed as $M_1 = 1.40\,M_\odot$ (Cox & Pilachowski 2000), and $M_2 = 0.97\,M_\odot$.

In the $O - C$ diagram shown in Figure 3, the long-term decrease in period and cyclic oscillation were derived. The orbital period of V680 Per is decreasing at a rate of $dP/dt = -8.16 \times 10^{-8}$ d yr^{-1}. With the secular decrease in period, the degree of overcontact will become higher. Therefore, this system will evolve into a deeper overcontact binary, if the decrease in orbital period is due to conservative mass transfer from the more massive component to the less massive one. By considering a conservative mass transfer equation from the primary to the secondary (Singh & Chaubey 1986),

$$\frac{\dot{P}}{P} = 3\dot{M}_2(\frac{1}{M_1} - \frac{1}{M_2}), \quad (4)$$

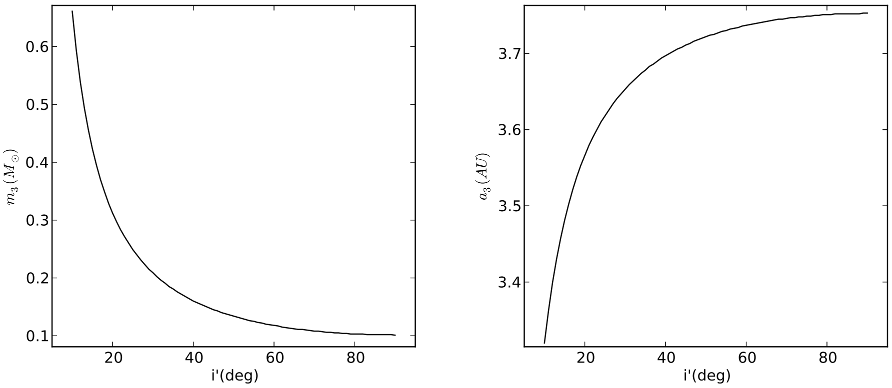

Fig. 7 The mass and orbital inclination for an assumed third body in V680 Per.

the mass transfer at a rate of $dM_2/dt = 2.30 \times 10^{-7}\,M_\odot\,\mathrm{yr}^{-1}$ was determined. Therefore, the long-term decrease may result from conservative mass transfer from the more massive star to the less massive one, or angular momentum loss due to magnetic stellar wind.

Cyclic oscillations in the $O - C$ diagram are usually explained by the light-travel time effect via the presence of a third body (Liao & Qian 2010; Zhu et al. 2013a,b; Qian et al. 2011, 2012, 2015). With the same method as used by Zhu et al. (2013a,b), the relations between semi-major axis of the third body, and of the third body mass, and the orbital inclination for an assumed third body in V680 Per are depicted in Figure 7. The estimated mass of the third body is $M_3 \sin i' = 0.101\,M_\odot$. If the orbital inclination i' is 90°, the mass of the third body should be $m_3 = 0.101\,M_\odot$ with the maximal orbital radius of $a_3 = 3.75$ AU. During the photometric solutions, we also searched for the contribution of the third body to the total light of the system, but the value of L_3 was always negative. Thus, the third body may be a very faint main sequence case.

Moreover, it is necessary for us to obtain many high-precision photometric and spectroscopic observations of V680 Per, in order to detect magnetic activities and determine the system's absolute parameters much more precisely.

Acknowledgements The CCD photometric observations of V680 Per were obtained with the 1.0-m and 60-cm telescopes managed by Yunnan Observatories and with the 85-cm telescope at Xinglong Station of National Astronomical Observatories. This work is supported by the Joint Research Found (Nos. U1831109 and U1631108) in Astronomy under cooperative agreement between the National Natural Science Foundation of China (NSFC) and Chinese Academy of Sciences (CAS), the Science Foundation of China University of Petroleum-Beijing at Karamay (Nos. RCYJ 2016B-03-004 and 2016B-03-006) and Key Laboratory for the Structure and Evolution of Celestial Objects, Chinese Academy of Sciences (No. OP201708).

References

Bradstreet, D. H., & Guinan, E. F. 1994, in Astronomical Society of the Pacific Conference Series, 56, Stellar Mergers and Acquisitions: The Formation and Evolution of W Ursae Majoris Binaries, ed. A. W. Shafter, 228

Cox, A. N., & Pilachowski, C. A. 2000, Physics Today, 53, 77

Diethelm, R. 2010, Information Bulletin on Variable Stars, 5920, 1

Diethelm, R. 2011, Information Bulletin on Variable Stars, 5960, 1

Diethelm, R. 2012, Information Bulletin on Variable Stars, 6011, 1

Diethelm, R. 2013, Information Bulletin on Variable Stars, 6042, 1

Drake, A. J., Djorgovski, S. G., Mahabal, A., et al. 2009, ApJ, 696, 870

Faulkner, D. R., Samec, R. G., Hawkins, N. C., et al. 2004, in American Astronomical Society Meeting Abstracts, 205, 18.04

Gettel, S. J., Geske, M. T., & McKay, T. A. 2006, AJ, 131, 621

Guinan, E. F., & Bradstreet, D. H. 1988, in NATO Advanced Science Institutes (ASI) Series C, 241, eds. A. K. Dupree, & M. T. V. T. Lago, 345

He, J., & Qian, S. 2009, Ap&SS, 321, 209

Hubscher, J., & Lehmann, P. B. 2012, Information Bulletin on Variable Stars, 6026, 1

Irwin, J. B. 1952, ApJ, 116, 211

Kallrath, J & Milone, E. F. 1999, Eclipsing Binary Stars: Modeling and Analysis (New York: Springer)

Krajci, T. 2006, Information Bulletin on Variable Stars, 5690, 1

Liao, W. P., & Qian, S. B. 2010, MNRAS, 405, 1930

Liao, W. P., Qian, S. B., Zhao, E. G., & Jiang, L. Q. 2014, New Astron., 31, 65

Lucy, L. B. 1967, ZAp, 65, 89

Nelson, R. H. 2009, Information Bulletin on Variable Stars, 5875, 1

Nelson, R. H. 2010, Information Bulletin on Variable Stars, 5929, 1

Qian, S. B., Liu, L., Liao, W. P., et al. 2011, MNRAS, 414, L16

Qian, S. B., Liu, L., Zhu, L. Y., et al. 2012, MNRAS, 422, L24

Qian, S. B., Zhou, X., Zola, S., et al. 2014a, AJ, 148, 79

Qian, S. B., Wang, J. J., Zhu, L. Y., et al. 2014b, ApJS, 212, 4

Qian, S. B., Han, Z. T., Fernández Lajús, E., et al. 2015, ApJS, 221, 17

Qian, S.-B., He, J.-J., Zhang, J., et al. 2017, RAA (Research in Astronomy and Astrophysics), 17, 087

Ruciński, S. M. 1969, Acta Astronomica, 19, 245

Rucinski, S. M. 1997, AJ, 113, 1112

Samec, R. G., Hawkins, N. C., Miller, J., et al. 2005, Information Bulletin on Variable Stars, 5610, 1

Singh, M., & Chaubey, U. S. 1986, Ap&SS, 124, 389

Sterken, C. 2005,in Astronomical Society of the Pacific Conference Series, 335, Ole Roemer and the Light-Time Effect, ed. C. Sterken, 181

Van Hamme, W., & Wilson, R. E. 2007, ApJ, 661, 1129

Wilson, R. E. 1979, ApJ, 234, 1054

Wilson, R. E. 1990, ApJ, 356, 613

Wilson, R. E. 2008, ApJ, 672, 575

Wilson, R. E., & Devinney, E. J. 1971, ApJ, 166, 605

Zejda, M. 2002, Information Bulletin on Variable Stars, 5287, 1

Zejda, M. 2004, Information Bulletin on Variable Stars, 5583, 1

Zejda, M., Mikulasek, Z., & Wolf, M. 2006, Information Bulletin on Variable Stars, 5741, 1

Zhou, A.-Y., Jiang, X.-J., Zhang, Y.-P., & Wei, J.-Y. 2009, RAA (Research in Astronomy and Astrophysics), 9, 349

Zhu, L.-Y., Qian, S.-B., & Xiang, F.-Y. 2004, PASJ, 56, 809

Zhu, L., & Qian, S. 2006, MNRAS, 367, 423

Zhu, L. Y., Qian, S. B., Liu, N. P., Liu, L., & Jiang, L. Q. 2013a, AJ, 145, 39

Zhu, L. Y., Qian, S. B., Zhou, X., et al. 2013b, AJ, 146, 28